

# Supplementary material for Surface spin fluctuations probed with flux noise and coherence in Josephson phase qubits

Daniel Sank<sup>1</sup>, R. Barends<sup>1</sup>, Radoslaw C. Bialczak<sup>1</sup>, Yu Chen<sup>1</sup>, J. Kelly<sup>1</sup>, M. Lenander<sup>1</sup>, E. Lucero<sup>1</sup>, Matteo Mariantoni<sup>1,5</sup>, M. Neeley<sup>1,4</sup>, P.J.J. O'Malley<sup>1</sup>, A. Vaisencher<sup>1</sup>, H. Wang<sup>1,2</sup>, J. Wenner<sup>1</sup>, T.C. White<sup>1</sup>, T. Yamamoto<sup>3</sup>, Yi Yin<sup>1</sup>, A.N. Cleland<sup>1,5</sup>, and John M. Martinis<sup>1,5\*</sup>

<sup>1</sup>*Department of Physics, University of California, Santa Barbara, California 93106-9530, USA*

<sup>2</sup>*Department of Physics, Zhejiang University, Hangzhou 310027, China*

<sup>3</sup>*Green Innovation Research Laboratories, NEC Corporation, Tsukuba, Ibaraki 305-8501, Japan*

<sup>4</sup>*Lincoln Laboratory, Massachusetts Institute of Technology, Lexington, MA 02420-9108 and*

<sup>5</sup>*California NanoSystems Institute, University of California, Santa Barbara, CA 93106-9530, USA*

(Dated: November 16, 2011)

Here we present experimental details on the Ramsey Tomography Oscilloscope (RTO) protocol and details of the calculations used to extract the flux noise magnitude from Ramsey decay data.

## RAMSEY TOMOGRAPHY OSCILLOSCOPE

Here we describe the data processing procedure for the Ramsey Tomography Oscilloscope (RTO). We found that careful signal processing was important in reducing statistical noise in the power spectra generated by the RTO. The bandwidth of the RTO measurement is set fundamentally by the rate at which the qubit can be measured and reset. In our case this would allow ideally 10,000 quantum measurements per second. With our current asynchronous control software this limit could not be reached while simultaneously tracking the time at which each measurement occurred. Maximum data rate with accurate time stamping was achieved with 2,400 quantum measurements per second, 600 of each of the four tomography sequences. Averaging the 600 measurements together produced one frequency measurement per second. This set the bandwidth of the experiment to be 0.5 Hz due to the Nyquist criterion.

Data was typically acquired for eight to ten hours, yielding between 28,000 and 36,000 points in the time series. Power spectra are computed as follows. First, the time series is divided into four or five non-overlapping sections. We compute the power spectrum of each section separately and average them together at the end of the procedure. To eliminate uncorrelated quantum measurement shot noise, we use an interleaving procedure on each section. Each section is split into two interleaved time series,  $f_1(n)$  and  $f_2(n)$  ( $n$  is the discrete time index). These series are multiplied by Hann windows and the discrete Fourier transforms  $F_1(k)$  and  $F_2(k)$  are computed ( $k$  is a frequency bin index). We form the product  $F_1(k)F_2^*(k)$ , average neighboring bins together using a Gaussian weight function with full width at half maximum (FWHM) of 20 bins, and take the magnitude to obtain the periodogram  $P(k)$ . Next, the periodogram is multiplied by a factor  $1/0.375$  to correct for the loss of incoherent (noise) power caused by application of the Hann window [1]. The periodogram is then smoothed by averaging neighboring frequency bins with a Gaussian

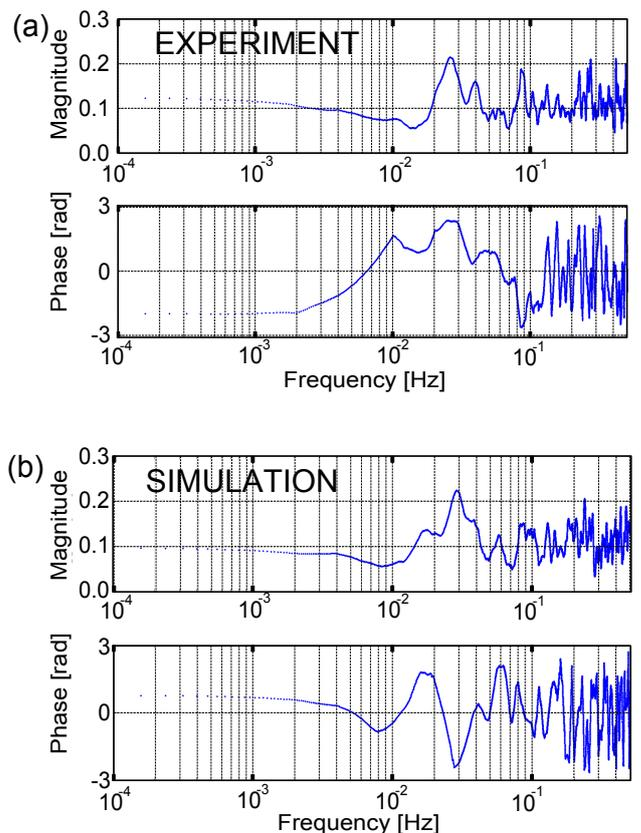


Figure 1: Cross spectra. (a) Cross spectrum measured using the RTO. (b) Cross spectrum computed from two independently simulated  $1/f$  noise signals.

weight function with a variable FWHM scaling quadratically from 1 bin at the low end of the frequency band to 20 bins at the high end. The power spectrum  $S(f)$  is then computed from the periodogram according to

$$S(f) = \frac{2T}{(N/2)^2} P(k = fT) \quad (1)$$

where  $T$  is the total length of time represented by the section of the time series, and  $N$  is the number of points in

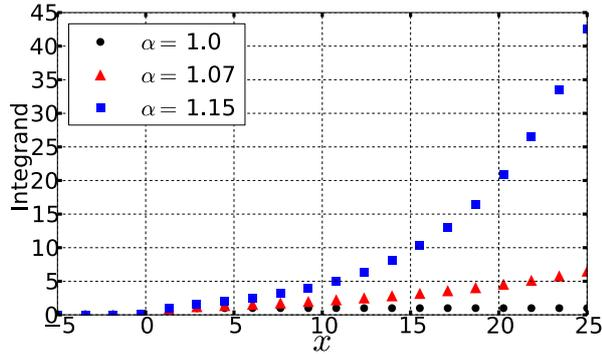


Figure 2: (color online) The integrand of  $I$ . The curves are well behaved over the entire integration range.

the section. Finally, spectra generated from each section are averaged together.

### CROSS CORRELATION

In order to check that the flux noise we measured was generated locally to each device, we used the RTO to measure cross correlation of the noise signals generated in two devices separated by  $500 \mu\text{m}$  on the same chip. Time series of the two devices' resonance frequencies were measured using the RTO, and the cross correlation was computed. Results are shown in Fig. 1. Although there are frequencies at which the cross correlation amplitude is as high as 0.3, this must be compared against the cross correlation computed for two independently simulated noise signals. We find that the cross correlation of two independently simulated  $1/f$  noise signals show very similar peak structure to the data, indicating that the noises within the two qubits are no more correlated than independent noise. This result agrees with the finding in Ref. [2], where it was inferred from quantum state tomography performed on two coupled qubits that dephasing in each qubit was uncorrelated. We note that the absence of a low frequency roll-off in the RTO data indicates that the low frequency flux noise is correlated on time scales exceeding the length of data acquisition. For this reason it is unsurprising that residual cross-correlation was found in both the data and the simulation.

### COMPARISON OF RTO AND RAMSEY DECAY

We wish to fit our Ramsey decay data to the theoretical curve given by Eq. (1) in the main text, which, for the

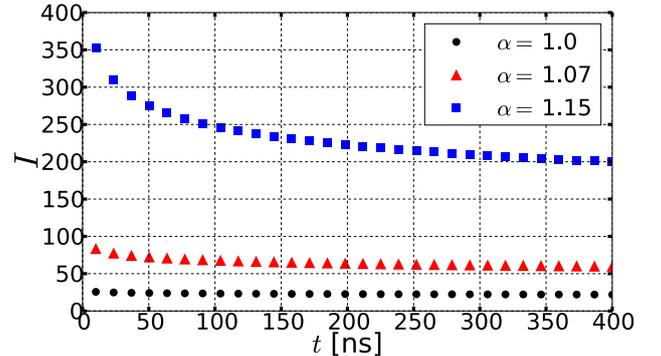


Figure 3: (color online) The integral  $I$  evaluated versus  $t$  for several values of  $\alpha$ . Note the strong sensitivity to  $\alpha$ ; as  $\alpha$  goes from 1.0 to 1.15, a 15% change, the integral increases by a factor of  $\sim 10$ .

case where the flux noise is  $S_{\Phi}(f) = S_{\Phi}^*/f^{\alpha}$ , is

$$p(t) = \exp \left[ -\frac{(2\pi)^2}{2} \left( \frac{df_{10}}{d\Phi} \right)^2 S_{\Phi}^* t^{1+\alpha} \int_{f_m}^{\infty} \frac{\sin(\pi z)^2}{(\pi z)^2} \frac{dz}{z^{\alpha}} \right] \quad (2)$$

Here  $\text{sinc}(x) \equiv \sin(x)/x$ ,  $f_m \approx 1$  hour and  $t$  is in the range 0 to 400 ns [4]. In order to do this we need to evaluate the integral

$$I = \int_{f_m t}^{\infty} \frac{\sin(\pi z)^2}{(\pi z)^2} \frac{dz}{z^{\alpha}}. \quad (3)$$

We compute the integral numerically. Since  $f_m t$  is on the order of  $10^{-12}$ , the lower limit of integration is a very small positive number and the integrand is diverging at the lower limit. On the other hand, the integrand oscillates for  $z > 1$ . The integral is therefore unfit for numerical analysis in its current form as it has both divergent and oscillatory behavior. The problem is mitigated by the change of variables  $x \equiv -\ln(z)$  which yields

$$I = \int_{-\infty}^{-\ln(f_m t)} \frac{\sin(\pi e^{-x})^2}{(\pi e^{-x})^2} \frac{dx}{e^{x(\alpha-1)}} \quad (4)$$

The integrand is now well conditioned over the whole integration range. Plots of this integrand for several values of  $\alpha$  are shown in Fig. 2. Note that an upper cutoff in the frequency integral would translate to a lower cutoff in the integral over  $x$ . Because of the logarithmic scale combined with the very small value of the integrand for values of  $x \leq 5$ , ignoring a possible upper cutoff greater than 1 MHz incurs negligible error.

We perform the integral  $I$  for 50 values of  $t$  in the experimental range 0 to 400 ns, and for several values of  $\alpha$  near 1. Results of the integration as a function of  $t$  are shown in Fig. 3. We also show  $I$  as a function of  $\alpha$  for two fixed values of  $t$  in Fig. 4. From these curves we construct interpolating functions and use them to fit our

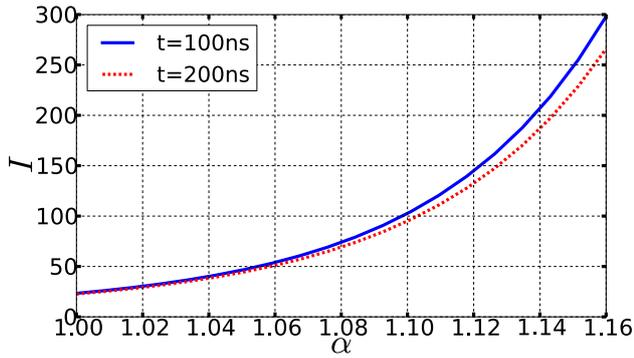


Figure 4: (color online) The integral  $I$  evaluated as a function of  $\alpha$  for several values of  $t$ . Note the strong dependence on  $\alpha$ .

measured Ramsey decay data to Eq.(2). Note particularly in Fig. 4 the strong dependence of the noise integral on  $\alpha$ . It is because of this strong dependence that we are able to accurately determine which value of  $\alpha$  gives the

best agreement with the power spectra measured directly using the RTO, as described in the main text.

---

\* Electronic address: [martinis@physics.ucsb.edu](mailto:martinis@physics.ucsb.edu)

- [1] F. J. Harris, Proc. IEEE **66**, 51 (1978).
- [2] R. C. Bialczak et al., Nature Phys **6**, 409 (2010).
- [3] D. J. Van Harlingen, T. L. Robertson, B. L. T. Plourde, P. A. Reichardt, T. A. Crane, and J. Clarke, Phys. Rev. B **70**, 064517 (2004).
- [4] The lower cutoff frequency  $f_m = 1/\text{hour}$  arises from the manner in which we acquire the data. Because we use a projective quantum measurement to read the state of the qubit, we must repeat the experiment for each value of  $t$  many times to reduce statistical noise. Rather than average each point in  $t$  sequentially, we spread the averaging of each point over the entire trace acquisition period. This results in better averaging of the noise signal as explained in Ref. [3].